Heat transfer correlations and pressure drop dynamics of palm fibre wetting media for evaporative cooling at different air flow rates

Ndukwu M.C[a], Mathew I Ibeh, Godwin Edem Akpan, Linus Oriaku, Ugochukwu Abada, Kalu C.A, Augustine Edet Ben, Jude Mbanasor, Hongwei Wu

Abstract

The thermal and flow resistance properties of wetting pads play a key role in how effective direct evaporative cooling (DEC) systems Perform. To make an informed decision, it's crucial to study the heat transfer properties and airflow resistance manifested in pressure drop for various types of wetting media. An experimental study was conducted to determine pressure drop and heat transfer correlation constants at three airflow rates for palm fruit mesocarp fibres (PFMF) wetting media. Heat transfer and pressure drop equations were fitted with generated data to obtain correlation constants. The wetting media were effective to lower the ambient temperature at an average depression of 6.6 to 8.2oC and increase the relative humidity of the inlet air at an average value of 25.54 to 39.32 %. PFMF had a low-pressure drop per unit length, ranging from 5.29 to 7.62Pa/m, which makes it an appealing alternative to other wetting media. New correlation constants generated for pressure drop and heat transfer data fit well with high coefficient of determination (R2) values. The average cooling efficiency ranged from 56.43 to 65.27%, while the average Merkel number was 0.16 to 0.19. The Nusselt number increased with the Reynolds number and showed a laminar flow. Amaranths stored in DEC produced respiratory heat ranging from 290.86 to 336.53mg/kg/h for all air velocities. Considering the respiratory rate within the range of cooler temperatures, it is recommended to use the DEC only for short periods or for pre-cooling of vegetable storage.

Introduction

Vegetables are highly perishable immediately once harvested (Ndukwu et al., 2022a). After harvest, they suffer a loss of moisture due to continuous breathing and if left unchecked, will result in wilting in vegetables and eventual decay due to microbes. Thus postharvest losses pose a serious challenge to the profit merging of farmers. Cooling has been the traditional means of extending the shelf life of fruits and vegetables but the lack of improved cooling or storage facilities in most rural areas increases post-harvest losses (Munoz et al., 2017). In most developing countries, the situation is made worst due to low electricity penetration density to power mechanical cooling devices and in some cases, the subsistence farming methods results in a low-income generation to acquire storage facilities (Kasso and Bekele, 2015). Again for developed economies and farmers that can afford mechanical compression cooling devices, energy conservation and energy-efficient systems are of common interest. Among energy-consuming applications, the deployment of energy in cooling systems is among the highest energy consumer globally (Ndukwu and Manuwa, 2015; Ndukwu et al., 2019 and 2022b). This high-level energy consumption generates massive greenhouse gases that damage the environment. Thus different research is looking for ways to provide alternative cooling devices that are cost-effective and environmentally sustainable to assist farmers and households in food and crop storage (Ndukwu et al., 2023). Among these devices, evaporative coolers have been used as energy-efficient and environmentally sustainable pre-cooler or storage systems in the cooling or storage of fruits and vegetables. Thus Lal Basideya et al (2011) has stated that evaporative coolers can save between 40-50% of the energy cost in the storage of crops. Therefore, different designs of evaporative coolers exist in the literature among which the direct and indirect evaporative cooling design is the most common (Ndukwu and Manuwa 2014; Liu et al., 2019). However, the principle of operation of an indirect evaporative cooler eliminates moisture from the supply air into the cooled environment or cold space. Thus both the temperature and relative humidity of the inlet air is lowered below the ambient. This makes this mode of evaporative cooling more suitable for housing comfort or data centres (Rao et al., 2020). In contrast the direct evaporative cooling the inlet air acquires moisture from the wetting media that increases its humidification before it enters the cooling space. Thus this makes this mode of evaporative cooling more suitable for the storage of fruits and vegetables because while the temperature of the inlet air is reduced, the humidity is increased. Fruits and vegetables require low temperatures and a highly humid environment to maintain their freshness. Thus direct evaporative cooling system being the most suitable has been used by researchers in the storage of fruits and vegetables. The design is very simple and affordable and the cost can be within the reach of rural farmers (Ndukwu and Manuwa, 2014, Ghani et al 2019). Hence, Nkoliza et al (2019) stored tomatoes in an evaporative cooler for 20 days and compared their performance with storage at room temperature and in a cold room. They concluded that for farmers in a rural areas, evaporative cooling storage provides the best storage alternatives. A storage life of 19 days was achieved by Islam and Morimoto (2019) in direct evaporative cooling storage of eggplants while Ambuko et al (2017) achieved a storage life of 8 days on amaranths leave using direct evaporative coolers. Similarly, Dalchi et al (2019) achieved a storage life of 3 to 5 days for various crops that include spinach, carrots etc while Ndukwu (2011) achieved a storage life of 19 days on tomatoes using a direct evaporative cooler. The above research showed the effectiveness of evaporative coolers in lowering the ambient temperature and increasing the relative humidity. One of the major components that act as this heat transfer sink is the wetting media and their performance is influenced by their thickness and air flow rate through it. It is the wetting media that absorbs and holds the water and the heat exchange between it and inlet air occurs before the air moves to the storage chamber to lower the environment (He et al., 2014, Yan et al., 2020). This wetting media add to the cost of evaporative coolers when artificial materials are used (Ndukwu et al., 2023). Therefore research has used biomass fibres (Eucalyptus fibre, Lufar, Khus etc) as an alternative to replacing company-manufactured wetting media which is expensive (Shekher et al., 2016; Aziz et al; 2018; Dogramacı et al, 2020). These biomass materials can be treated and made commercially available and their performance is a function of their heat transfer parameters under load (He et al 2014). This aspect of the study is still ongoing for different biomass fibres. One of the most abundant biomass fibres in Nigeria is palm fruit fibre because Nigeria is among the major producer of palm oil (Ndukwu and Asoegwu, 2010). In many oil mill industries, these fibres are treated as a waste product and discarded or burnt. This waste can be converted as wetting media and used in evaporative cooling. However, there is a need to study the heat transfer characteristics under load conditions in evaporative cooling preservation. Therefore the objective of this study is to investigate the influence of air flow rate on the pressure drop, water evaporation per unit temperature drop and non-dimensional correlations for heat transfer data in evaporative cooling storage of some fruits and vegetables using palm fruit fibre.

2. Material and methods

2.1 Cooling pad/Wetting media

In this study, we studied palm fruit Mesocarp fibre as the wetting media or cooling pad in the evaporative storage of amaranths. The fibre is a by-product of the milling and processing of palm fruit into palm oil. It is discarded as waste after palm fruit processing. The palm when obtained contains some leftover palm oil during palm oil milling and extraction. Thus the fibre was first washed with detergent to remove the oil and kill any germ available in it. After washing it was rinsed several times to remove the detergent and dried under the sun. The fibre was stretched to form strings and laid in heaps of 1m x 0.3m x 0.03 m with air spaces inside the pad holder which was fitted into the evaporative cooler.

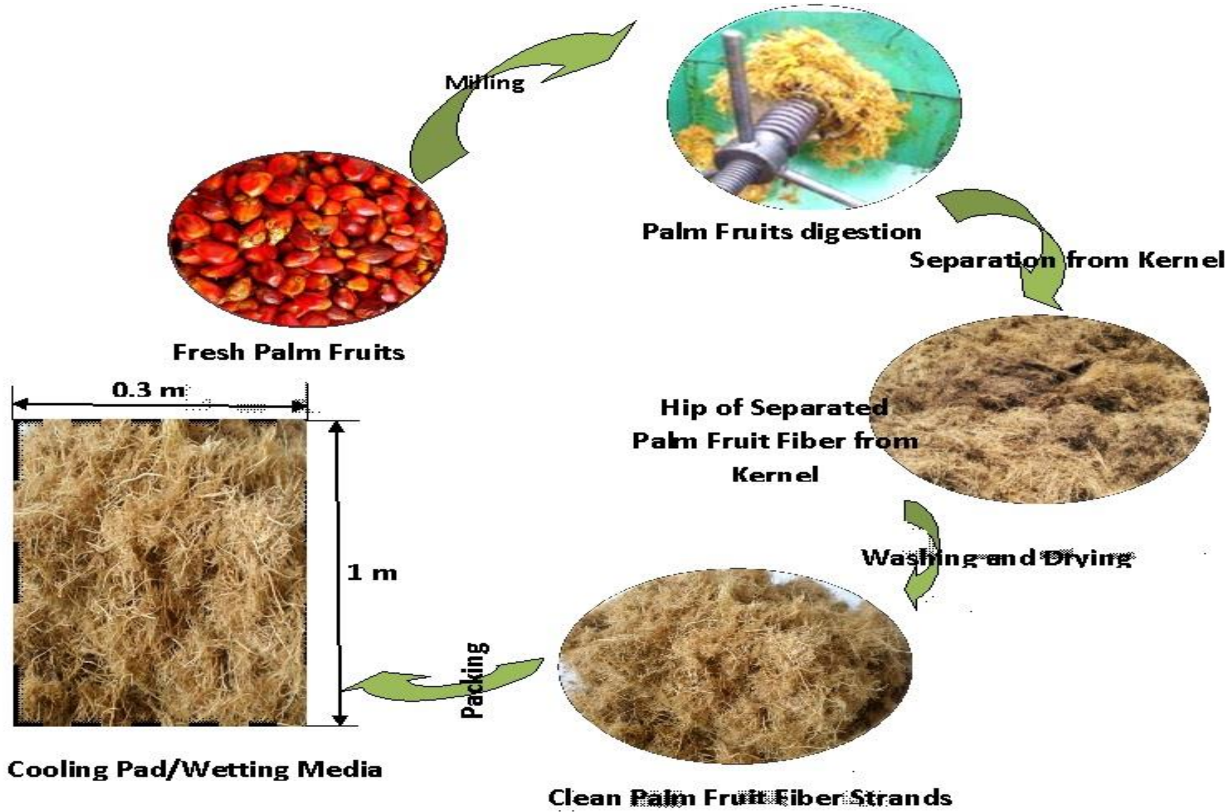

Figure 1: Preparation process of the palm fruit fibber cooling pad

2.3 Description and operation of the Standalone evaporative cooler

Figure 2 shows the pilot evaporative cooler utilized for the experiment. It is a stand-alone direct evaporative cooler (DEC) that was built locally in the university's student workshop. The DEC is made up of a delivery water tank (20 L) that is mounted on top of the storage tank and a sump water tank (20 L) that is placed beneath the storage tank. The storage chamber (0.24 m^3) is a double-jacketed hexagonal storage room with an aluminium sheet inner wall and galvanized steel sheet exterior wall. Fibreglass is installed between the walls to provide lagging. Figure 3 displays the evaporative coolers functioning schematics. A perforated header positioned horizontally on the edges of the wetting media receives water from the delivery tank at a flow rate of 10cm^3/s. The wetting media after saturation allows the saturated water to drain into a sump that is located just below the down edges of the wetting media after absorbing the water through capillary action and gravity until it becomes saturated. Under the cooling chamber, the sump tank has an opening into it. A sump water pump (0.075 kW) linked to the sump tank pumps water through a series of additional PVC pipes back to the delivery tank and the cycle continues. The inlet air flows across the wetting media with the help f three axial fans that can be placed inside or outs adjacent to the wetting media. An opening vent was present at the two ends on the top of the storage chamber for warm air to escape the storage room.

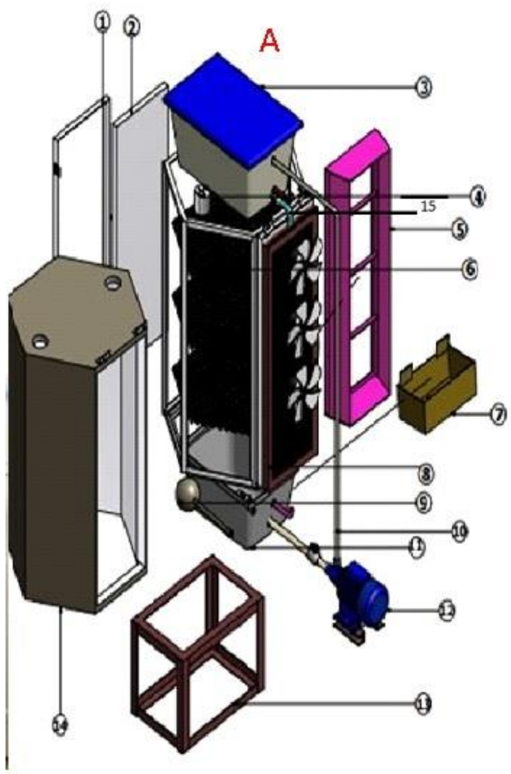

COMPONENTS OF THE EVAPORATIVE COOLING SYSTEM		
S/N	DESCRIPTION	QTY
1	DOOR FRAME	1
2	DOOR	1
3	UPPER WATER TANK	1
4	AIR VENT	2
5	AIR CHANNEL	1
6	FRUIT AND VEGETABLE TRAY	1
7	WATER COLLECTOR	1
8	COOLING PAD HOLDER	1
9	WATER CONTROL SWITCH	1
10	WATER RETURN PIPE	1
11	SUMP	1
12	WATER PUMP	1
13	STAND	1
14	COOLER HOUSING	1
15	WATER DISTRIBUTION HEADER	1

Figure 2. (A) Exploded view of the prototyped DEC showing the arrangements of the components (B) Front view of the picture of the developed DEC (C) Back view f the DEC

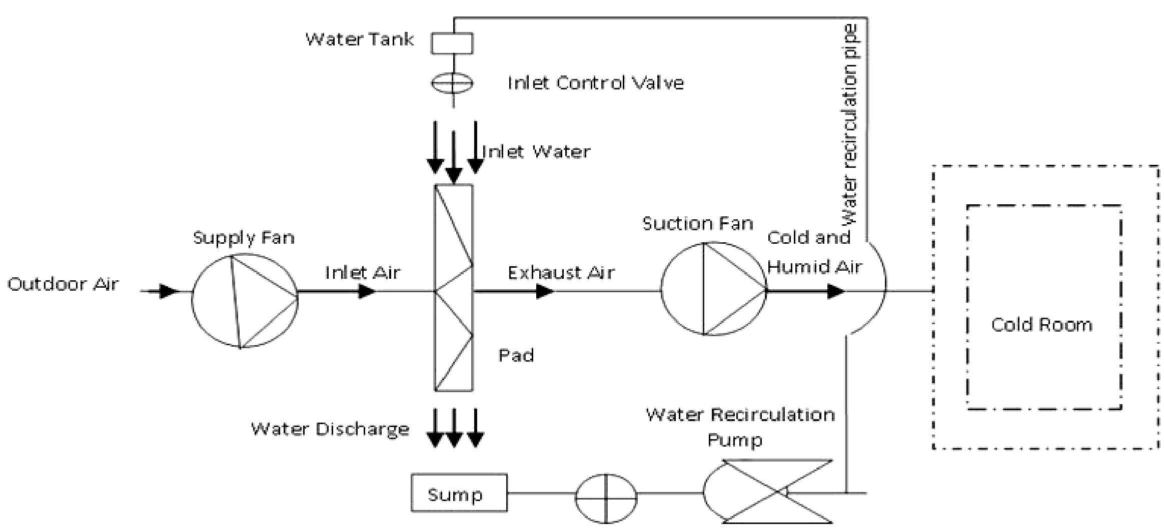

Figure 3: The scheme of operation of the pilot DEC

2.3: Data collection

The field experiment was carried out in February at three different air speeds of 3, 4 and 4,5 m/s. The DEC was used to store Amaranth leaves for seven days. The typical conditions of the amaranths leave during the storage and control are shown in Figure 4. The DEC was kept under an open shade to reduce the impact of solar radiation and to allow wind to cool down the delivery water stored in the delivery tank. The water delivery rate to the wetting media was determined as 1 x 10^{-5} m^3/s and this value was kept constant throughout the experiment. Before data collection, the DEC was switched on and allowed to operate several cycles until the wetting media is saturated with water. After which the fans were also switched on. The storage room was loaded with orange, paw-paw and amaranths leave. Measurement of the dry bulb, temperature, and relative humidity for the inlet and exit air was made with a thermocouple (K-type, USB linked; ±0. 1 ◦C) linked to a data logger (HH1147, ±0.1ºC and ±1 %, Omega Stanford USA). The measurements were logged in at a time interval of one hour. The ambient temperature and relative humidity were measured with a temperature-humidity clock (DTH-82; ±0.1 ºC, ±1.0 %, TLX, Guandong China) while the airspeed was measured with a vane anemometer (AM-4826, ±2% of the velocity; Landesk, Guangzhou, China).

Figure 4: conditions of the vegetables. A: Stored amaranths in DEC (48hrs), B: the state of the amaranths kept outside the cooler (48hrs), C: freshly harvested amaranths, D: the state of the amaranths kept outside the cooler (1 hr after harvest)

2.4 Theoretical analysis

Theoretically, direct evaporative cooling is referred to as adiabatic cooling because the sensible heat released by the air following humidification is close to the latent heat of water evaporation during the cooling of the input air. Hence, the water provided to the wetting media must be at a temperature that is closer to that of the wet bulb. Yan et al. (2021) assert that this is not the case in a system where the ambient conditions are uncontrolled and the delivery water tank is cooled by the wind and the movement is dependent on the weather, as in the current investigation. Therefore, by assuming the ideal gas condition in the energy balance at the air-vapour interphase and ignoring the variations due to little changes in the specific heat of water, He et al (2021) presented the sensible heat flux (Qs) as equation 1. Additionally using the log mean temperature they also presented the sensible heat flux (Qs) as equation 2. Thus combining equations 1 and 2, the heat transfer coefficient of evaporative cooled media can be presented as equation 3 as follows

$$Q_s = m_a C_{pa}(T_{in} - T_{out}) + m_a C_{pv}[X_{ain}(T_{in} - T_{wb}) - X_{out}(T_{out} - T_{wb})] \quad 1$$

$$Q_s = h_c A_s \Delta T_{lm} \quad 2$$

$$h_c = \frac{m_a C_{pa}(T_{in} - T_{out}) + m_a C_{pv}[X_{ain}(T_{in} - T_{wb}) - X_{out}(T_{out} - T_{wb})]}{A_s \Delta T_{lm}} \quad 3$$

C_{pa} is the specific heat capacity of air taken as 1.006 kJ/kg ^oC; C_{pv} is the specific heat capacity of water vapour taken as 4.18 kJ/kg ^oC at a temperature range of 19 - 40^oC, X is the specific humidity of the air, A_s is the area of the wetting material and ΔT_{lm} is the log mean temperature given as follows

$$\Delta T_{lm} = \frac{T_{in} - T_{out}}{\left[ln\frac{(T_{out} - T_{wb})}{(T_{in} - T_{wb})}\right]} \quad 4$$

We assume that the pad media is completely wet and the entire area of the cuboid-shaped pad is used in the heat transfer process. Thus we determine the heat transfer area (A_s) as the wetted pad area equivalent to an area of the cuboids with the same pad dimensions given as follows

$$A_s = 2(Lb + bh + Lh) \quad 5$$

Where b is the breath (m), L is the length (m), h is the height (m)

The mass flow rate (kg/s), $\dot{m}_a$ across the face of the wetting media is given as follows (Yan et al.2021)

$$\dot{m}_a = \rho_a v_a A_{mfs} \quad 6$$

Where v_a is the air speed (m/s), A_{mfs} is the cross-sectional area of airflow taken as the surface area (Length x breath) of the wetting media, *and* ρ_a is the density of moist air.

To determine the density of moist air, we assume that in evaporative cooling where the air flux around the cooling pad and the inlet water temperature is influenced by an uncontrolled ambient condition like the present design, the exit temperature is subjected to the variation in weather conditions and the amount of moisture absorbed. An increase in the moisture content of air decreases its density; hence the density of dry air is higher than that of moist air at the same pressure and temperature. Therefore in evaporative cooling higher ambient temperature causes higher moisture evaporation from the pad leading to dryer exit air (Ndukwu et al., 2023). Thus the density of exit air after humidification will vary with temperature as follows (Engineeringtoolbox.com)

$$\rho_a = \frac{\left(\frac{P_v}{R_a T}\right)(1+ X_{out})}{\left(1+\frac{X_{out} R_w}{R_a}\right)} \qquad 7$$

Where, R_a and R_w are gas constant of dry and water vapour given as 286.69 J/kgK and 461.5 J/kgK respectively, P_v is the vapour pressure (Pa) determined as follows (Ndukwu et al., 2019)

$$P_v = 610.8\, exp\left(\frac{17.27\, T}{T+273}\right) \qquad 8$$

Where T is the temperature (^oC) for inlet or outlet air

The specific humidity (X) is deduced as follows

$$X = \frac{\epsilon . P_v}{P_{atm} - P_{v.}.(1-\epsilon)} \qquad 9$$

Where P_{atm} is the atmospheric pressure taken as 101,325 Pa, ϵ is the gas constant ratio between wet and dry air given as 0.622 kg kg^{-1},

The wet bulb temperature (T_w) is determined as follows

$$T_w = T_{in} \times \arctan\left[0.151977 \times \sqrt{Rh + 8.313659}\right] + \arctan(T_{in} + Rh) - \arctan(Rh - 1.67633) + 0.00391838 \times (Rh)^{3/2} \times \arctan(0.023101 \times Rh) - 4.686035) \qquad 10$$

Where Rh is the relative humidity

The mass transfer coefficient (h_m) is deduced as follows

$$\frac{h_c}{h_m C_{p,a}} = Le^{2/3} = 1 \qquad 11$$

Where Le, is the Lewis number.

The heat transfer coefficient was used to determine the Nusselt number which is important heat transfer data for cooling medium evaluation as follows (Solhani et al., 2017)

$$\frac{Nuk}{h_c} = le \qquad 12$$

$$le = \frac{V}{A_s} \qquad 13$$

Where V is the volume of the pad, A_s is the heat transfer area, k is the conductive coefficient of air (0.025 W/m.K)

2.5 Specific water evaporation

Yan et al (2021) introduced the specific water evaporation (kg/(m.h. K) which they defined as hourly water evaporation at a unit thickness of the wetting media and a unit temperature change. It was given as follows

$$m_{sw} = \frac{\dot{m}_a(X_{out} - X_{in})}{l(T_{1n} - T_{out})} \times 3600 \qquad 14$$

2.6 Pressure drop

The pressure drop through the wetting media at different air velocities was determined empirically. It is assumed that as the temperature of exit air varies due to ambient conditions, the exit moist air density also varies which will affect the pressure drop across the pad as the time changes. Thus, using the empirical equation presented by Zhao et al (2023) for different cross-flow porous packing media and excluding the geometric length, the pressure drop was coupled directly with the mass velocity of air and water in equation 15 as

$$\Delta p = c{G_a}^a{G_w}^b \qquad 15$$

Where G_w and G_a are the mass velocity (kg/(m^2 s) of water and air respectively given in equations 16 and 17 as follows

$$G_w = \frac{\rho_w v_w}{A_w} \qquad 16$$

$$G_a = \rho_a \times u_a \qquad 17$$

Where ρ_a is the densities of air (kg/m^3) presented in equation w, and ρ_w is the density of water assumed at a constant value because the temperature variation with time was small, V_w and u_a are volumetric flow rate of water (m^3/s) and airspeed (m/s) while A_w is the cross-sectional area of wet surface

To obtain the value of the constant a, b and c in equation 15 we noticed that Zhao et al (2023) gave the values of a, in the range of 0.72 - 0.83, b in the range of 1.25 -1.31 and c, in the range of 0.98 - 1.01 for a cross flow porous packing. These values were given for six different kinds of porous packing media arrangements. Thus it was observed that these values are not statistically significant from each other when subjected to statistical analysis at a 95 % confidence limit. Hence for equation 16, we use the average value for a, b and c as 0.77±0.045, 1.27±0.024 and 0.99±0.014 respectively.

2.7 Cooling efficiency and Merkel number

The Merkel number and cooling efficiency are indices used to evaluate the performance of packing media (Zhao et al., 2023). The Merkel number implies that heat and mass transfer at the air-water interface is driven by the enthalpy difference while the cooling efficiency that is used is based on the limit of evaporative cooling. Thus equations 18 (Yilmaz, 2010) and 19 are used to determine the Merkel number and cooling efficiency as follows

$$Me = \frac{h_c A_s}{\dot{m}_a C_{p,a}} \quad 18$$

$$\eta = \frac{T_{1n} - T_{out}}{T_{in} - T_{wb}} \quad 19$$

The mass of water evaporated (m_w) is determined as follows

$$m_w = (X_{out} - X_{in})\dot{m}_a \quad 20$$

2.8 Determination of respiratory heat load of Amaranths

Respiratory heat load is another method of evaluating the performance of evaporative cooling performance. The lower the respiratory heat load, the longer the shelf life of the stored product. Thus the respiratory heat load variation with temperature is empirically determined with equation 21 as follows (Ndukwu et al., 2023)

$$q_{res} = \frac{10.7f}{3600}\left(\frac{9T}{5} + 32\right)^g \quad 21$$

Where T is the cooler temperature. For the respiratory coefficients f and g, we used the data presented in Becker and Fricke (1996) and respiratory heat load presented in USDA (1986) for spinach leave since they belong to the same plant family and are distant cousins with the same leave structure. Using the least square method at a storage temperature range of 20 and 21°C, the values determined for f and g were 4.89×10^{-4} and 4.47 respectively.

3. Results and Discussion

3.1 Influence of operation parameters and weather conditions

To investigate the influence of air flow rate on the operational parameters of the palm fruit mesocarp fibres under storage conditions with amaranths leave the time variations of the temperature and relative humidity difference are provided in figures 5 and 6 respectively for the three air velocities of 3, 4 and 4.5 m/s. These data were generated at varied air velocities when the volumetric flow rate of water was kept constant at $1x\ 10^{-5}$ m^3/s, with a determined media heat transfer area of 0.216 m and geometric length of 0.0215 m. The water temperature ranged from 18 to 25°C with an average value of 20°C with an inlet temperature ranging from 22.8 to 32.8 °C with a cooler temperature of 19.1 to 25.5 °C. These operational parameters were influenced by variations in weather conditions because the DEC was kept outside under an open shade. Thus the influence of wind is highly pronounced on the performance of the DEC (Ndukwu et al., 2023). It is noteworthy, that loading the DEC with the amaranth leaves also influenced the cooler temperature and relative humidity. The data in figure 5 and 6 showed that the wetting media coupled with the operational input parameters were effective to lower the ambient temperature at an average depression of 6.6 to 8.2°C and increase the humidity of the inlet air at an average value of 25.54 to 39.32 % for the three air velocity. Thus the key objective of the DEC with the wetting media was achieved.

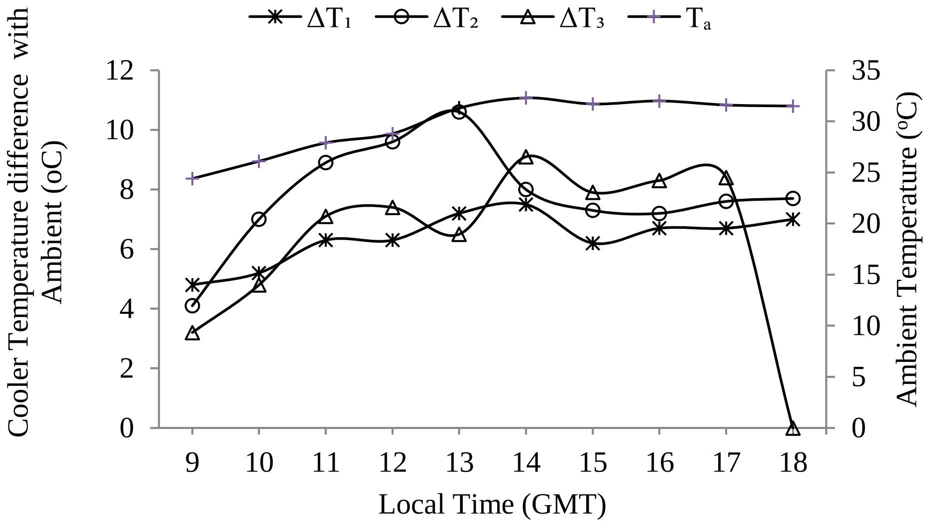

Figure 5: Temperature dynamics of the cooler: T_1 (4.5m/s), T_2 (4m/s), T_3 (3m/s), T_a (ambient temperature)

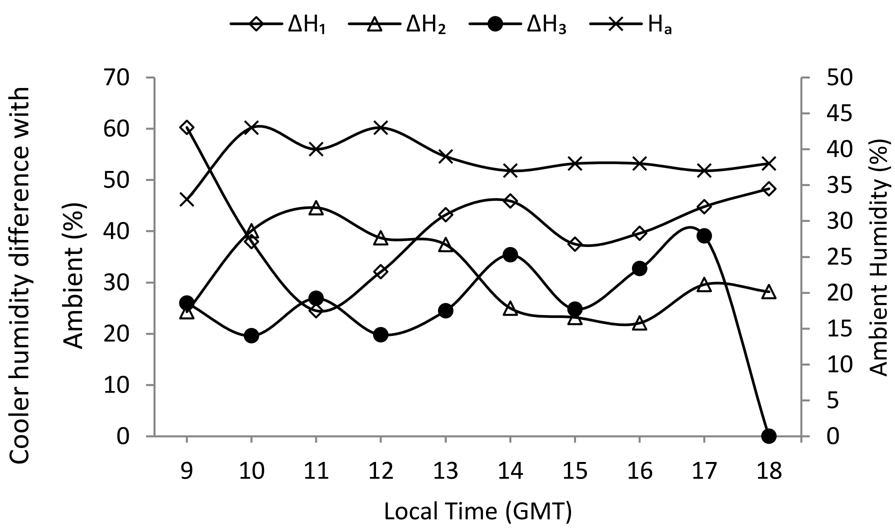

Figure 6: Humidity dynamics of the cooler: H_1 (4.5m/s), H_2 (4m/s), H_3 (3m/s), Ta (ambient temperature)

While temperature depression was higher at 4 m/s but humidification of the inlet air was higher at 4.5 m/s.

3.2 Specific water evaporation

Figure 7 showed that water evaporation per unit length and temperature changes is influenced by air velocity, humidity and ambient temperature (Ndukwu et al., 2022b). For the determination of the evaporation rate, the air mass flow rate varied according to $m_a = \rho_a \times u_a \times A_s$, however, it is assumed that the pad is fully wetted throughout the experiment; hence water flow rate does not influence the water evaporation rate though it was maintained at a constant value (He et al., 2014). Higher values were obtained at higher air velocity as shown in Figure 7 and this corresponds to other research in the literature

(Yan et al., 2021). Comparing figure 7 with the ambient temperature condition in figure 5 and relative humidity in figure 6, it shows that the water evaporation rate per unit length increased with an increase in temperature and decreased with the relative humidity of the inlet air.

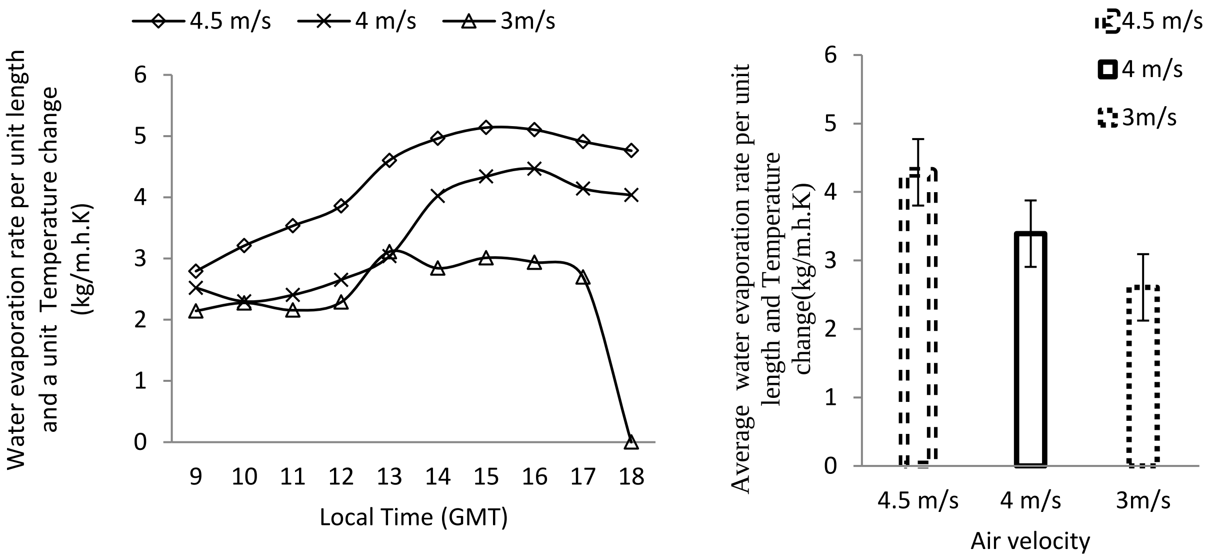

Figure 7: Water evaporation rate per unit length and temperature difference

3.3 Cooling efficiency, Merkel number and heat transfer coefficient

Cooling efficiency, heat transfer coefficient and Merkel number are important indexes used in the evaluation of the cold medium. Figure 8 showed the relationship between the cooling efficiency of the pad and the heat transfer coefficient with the temperature drop. The figure showed that increased temperature depression and decrease in heat transfer coefficient lead to increased cooling efficiency for the palm fruit wetting media. Although cooling effectiveness is affected by the media thickness, air velocity and ambient conditions, however in this case the media thickness was kept constant at 0.03m. The cooling efficiency ranged from 39.11 to 75.85 % for air velocity of 3m/s while it ranged from 27.74 to 75.86 % and 52.49 to 73.61% for 4 and 4.5 m/s respectively. However, on average, both the cooling efficiency and heat transfer coefficient ticked up slightly with air velocity within the range of tested air velocity, but the difference is not statistically different ($p < 0.05$) at 4 and 4.5 m/s. Zhao et al (2023) and Wang et al (2022) showed that packing methods can affect the cooling efficiency variation with air speed in wetting media at a constant water flow rate. Thus they corroborated our findings that cooling efficiency can increase with air velocity in direct evaporative cooling. However, the maximum cooling efficiency in the range of obtained values was calculated at the lowest air velocity of 3 m/s. Therefore reducing the airflow velocity or increasing the thickness of the wetting media is likely to enhance the cooling efficiency of palm fruit fibre. The average heat transfer coefficients were 17.47, 20.93 and 23.28 $W/m^2.K$ respectively.

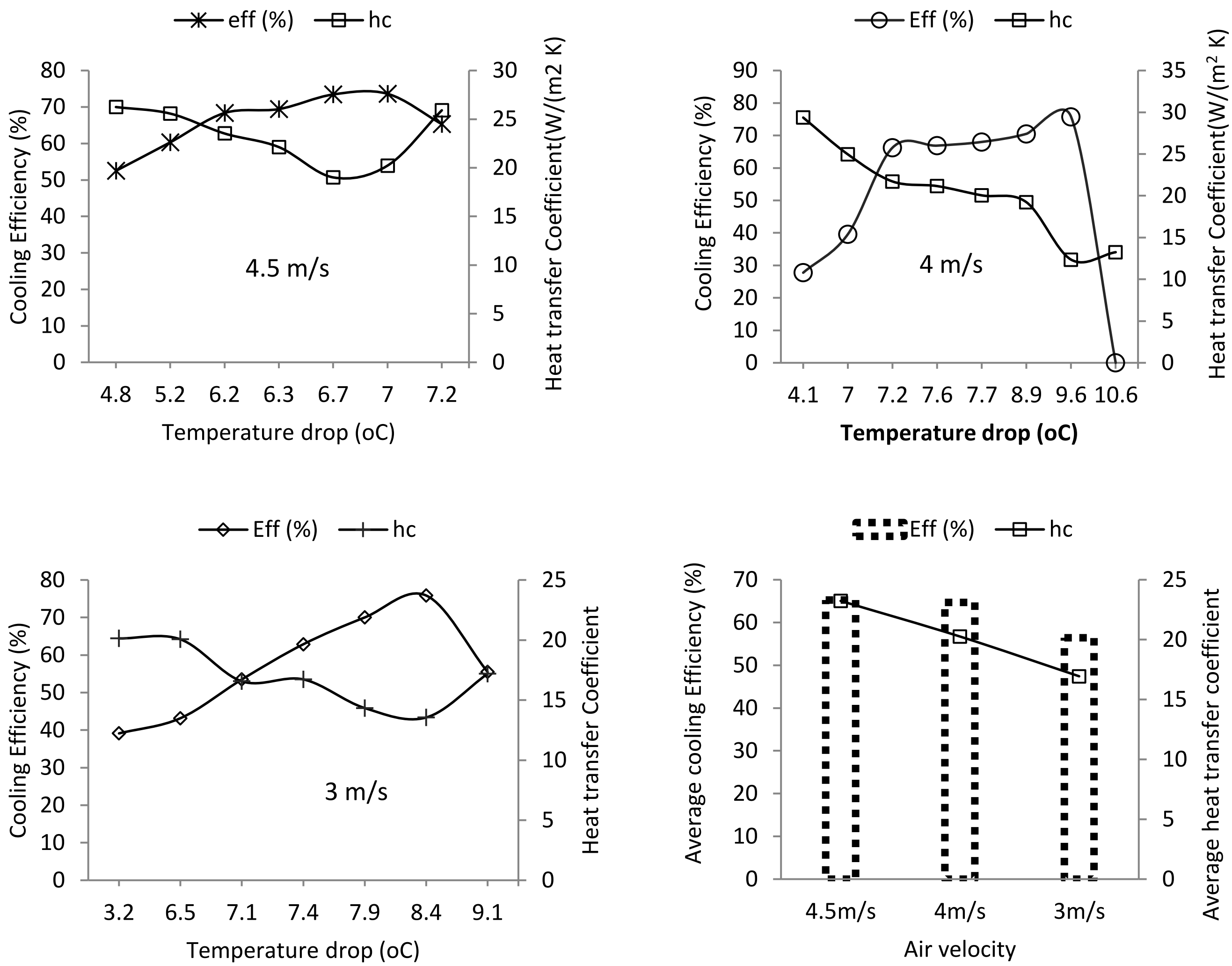

Figure 7: Cooling efficiency and heat transfer coefficient variations with temperature difference

Merkel's theory is also known as the enthalpy difference theory and the Merkel number is a good evaluation index in the evaporative cooling study. Using equation 22 the Markel's number for different airflow conditions are determined and the relationship between the Markel number and air velocity at different time variation is presented in Figure 8. The Markel number seems to, decreased with time as a result of a temperature rise when you compare Figure 8 with the ambient temperature in Figure 5, though this trend is irregular from the figure. The reason adduced by Zhao et al (2023) for this is due to a decrease in the air-to-water ratio (m_a/m_w) as a result of higher water evaporation at a higher temperature. This relationship can be represented with equation 22 according to Goshayshi and Missenden (200) for palm fruit fibre with constants in Table 3. However, as observed by Zhao et al (2023), the trend of Markel number variation increased with air velocity unlike cooling efficiency in figure 7 but the higher the Merkel number the higher the mass transfer rate and the more efficient the heat and mass transfer performance of the media. Equation 23 showed the empirical relationship of the heat transfer coefficient with the Merkel number from the experiment with the constants presented in Table 3.

$$M_e = k_1 \left(\frac{\dot{m}_a}{\dot{m}_w}\right)^{k_2} \quad 22$$

$$M_e = \left(k_1 + k_2 {h_c}^{k_3}\right)^{-1} \quad 23$$

Table 3; Constants for equation 22 and 23

Equation	Constants			
	k_1	k_2	k_3	R^2
20	0.06847	0.17933	-	1.0000
27	5.95	-4.92×10^{-13}	8.39	0.99992

Figure 8 showed that the highest Merkel number was obtained at 3 m/s while the lowest was obtained at 4.5 m/s. In terms of system cooling efficiency, the result of the Markel number showed an inverse relationship with cooling efficiency.

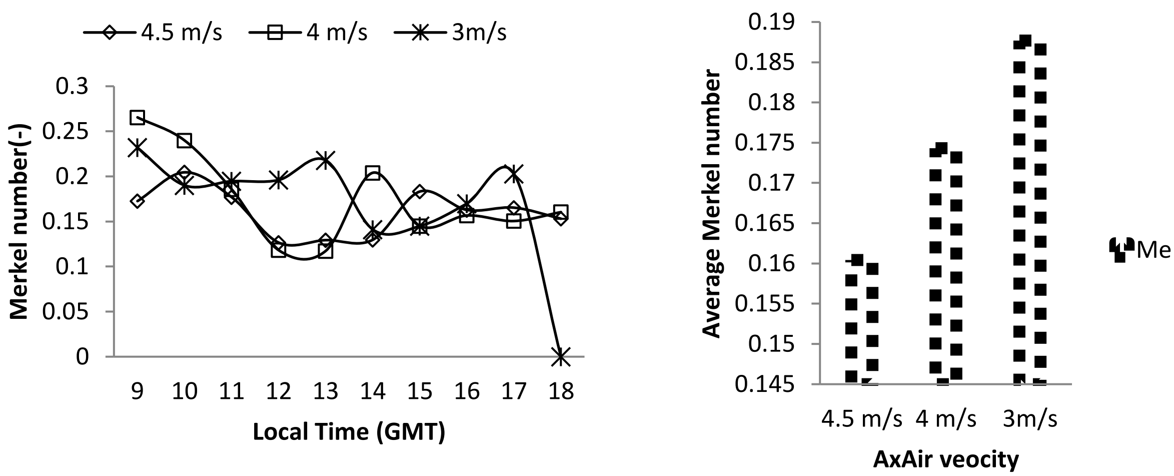

Figure 8: Merkel number variation with time and air velocity

3.4 Pressure drop dynamics of the wetting media

Figure 9 shows the pressure drop per unit length of the wetting media at different air velocities and temperature drops. The pressure drop shows the resistance overcome in the gas phase during the passage of the gas-liquid medium through the thickness of the cooling pad (Wang et al., 2022). Generally, the pressure drop is influenced by pad thickness, water and air flow velocity but in this research, the airflow velocity was varied at a constant pad thickness of 0.03m. Thus the pressure drop per unit length decreased with a decrease in air velocity and an increase in temperature drop which is consistent with studies in the literature (Milli et al., 2011, Wang et al., 2022). From the data the average pressure drop per unit length across the pads for all flow rates ranged from 5.29 to 7.62 Pa/m which is very low for a pad thickness of

0.03m, therefore it will be beneficial in adopting the palm fruit mesocarp fibre as a cooling pad in DEC. Furthermore, research has shown that the relationship between the mass velocity of air and water is exponential as shown in equation 16. Thus to test our obtained data, we regressed, the entire pressure drop for the three air velocities with the volumetric flow rate and density of the exit air according to equation 24 which has been used in literature (Franco et al., 2010; He, et al., 2014, Yan et al., 2021) and the constants determined for palm fruit fibre mesocarp wetting media are presented in Table 4

$$\Delta p = a\left(\frac{le}{l}\right)^{b}\left(1 + c\,\frac{q_w}{q_a}\right)\left(\frac{\rho_a u_a^2}{2}\right) \qquad 24$$

Table 4: constants in equation 20 and 21

Equation	Constants			
	a	b	c	R^2
24	1.12012	0.0317	0.91247	0.98885
25	2.11233	0.96116	-	0.98885

For equation 27, He et al (2014) and Yan et al., (2021) separated the mass velocity by introducing the volumetric flow rate of air (q_a) and water (q_w) in the pressure loss with the constant c. However, in this research, we modify equation 24 by removing the constant c and introducing the mass velocity directly in the pressure loss correlation in equation 28. The aim is to reduce the number of constants in the equations. Hence the values of pressure drop were also fitted with mass flow velocity with equation 25 and the constants and coefficient of determination were also presented in Table 4.

$$\Delta p = a\left(\frac{le}{l}\right)^{b}\left(1 + \frac{G_w}{G_a}\right)\left(\frac{\rho_a u_a^2}{2}\right) \qquad 25$$

Currently, researchers are also investigating the effect of pressure drop on temperature correlations (Ma et al., 2022). As reflected in the simulation work of Ma et al (2022) the pressure drop decreased with an increase in inlet temperature. Thus based on the deduction in this work involving temperature drop and inlet temperature, it was observed that higher inlet temperature results in a higher temperature drop. Therefore from figure 9, the pressure drop in palm fruit mesocarp fibre increased with an increase in temperature which corresponds to a higher temperature drop. A regression correlation equation linking pressure drop, temperature drop per unit length and mass flow rate of air is presented in equation 26 with an R^2 value of 0.999 as follows

$$\Delta P^2 = \beta + \left(\frac{\Delta T}{l}\right)^{k} \times (\rho_a v_a A_s)^{\alpha} \qquad 26$$

Where β, k and α, are constants determined as -0.3876, 8.957×10^{-4}, and 0.3317 respectively

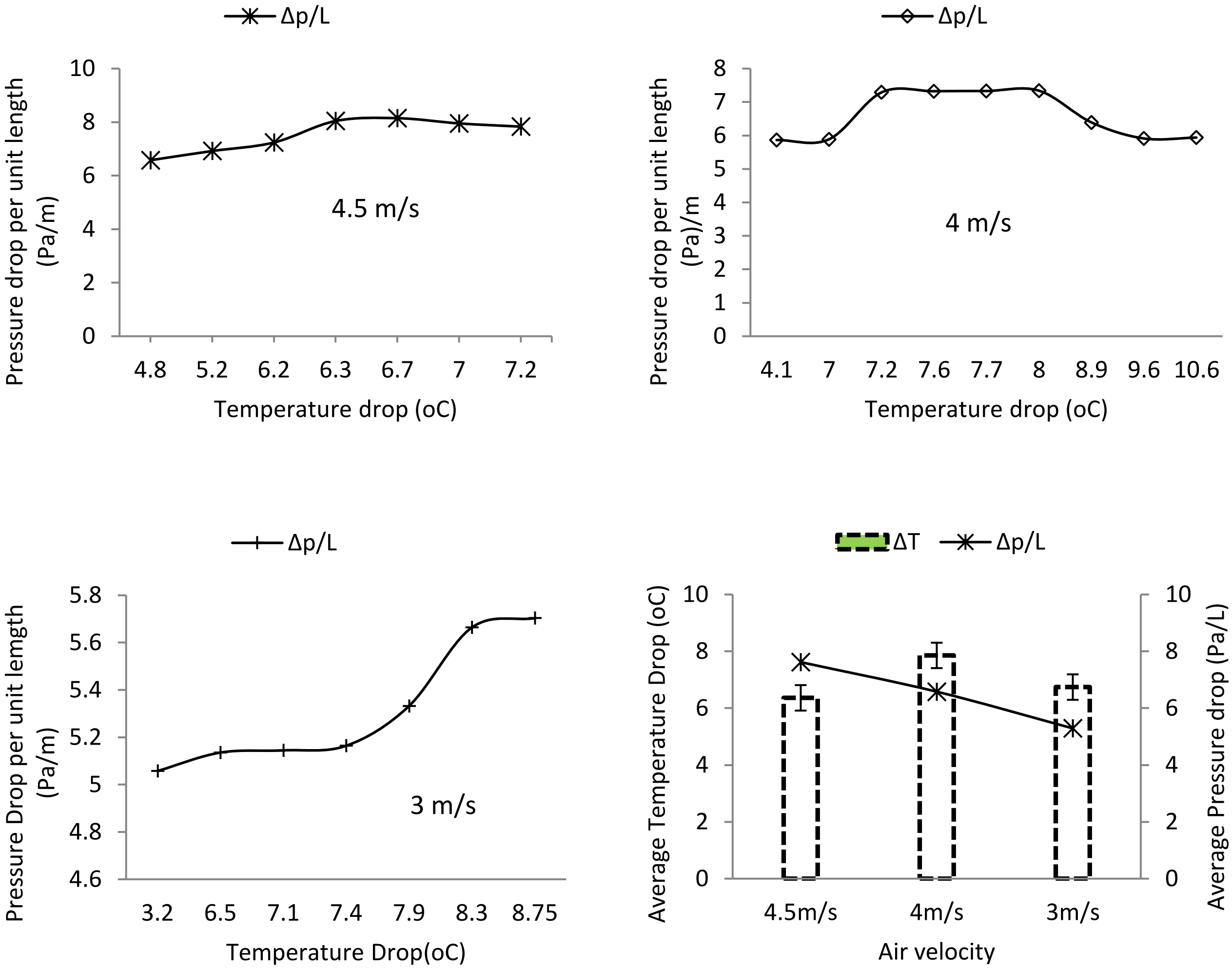

Figure 9: Pressure drop dynamics with Temperature changes at a different air velocity

3.5 Heat transfer correlations

The Nusselt number is important to heat transfer data for cooling medium evaluation. The heat transfer coefficient determined was used to calculate the Nusselt number. A low Nusselt number is an indication of lower heat transfer capacity (Solhani et al., 2017). From figure 10, the Nusselt number increased with the Reynolds number for all air velocities but when compared for each air velocity, they decreased with air velocity. Several correlations have been developed for the Nusselt number in the literature. Thus, to test our data and generate the constants for the palm fibre cooling pad, the data were fitted with equations 27 and 28 (He et al 2014) for DEC wetting media that shows the interconnectivity between heat transfer data and non-dimensional geometric factor

$$Nu = a\left(\frac{l_e}{l}\right)^b Re^c Pr^{1/3} \quad 27$$

$$Nu = a\left(\frac{l_e}{l}\right)^b \left(\frac{(T_{in}-T_{wb})}{T_w}\right)^c Re^d Pr^{1/3} \quad 28$$

Re is the Reynolds number ($\frac{u_a \rho_a le}{v} = Re$), Pr is the Prandtle number, T_w is the water temperature, *l* is the pad thickness (0.03 m), *le* is the geometric length

The constants for equations 27 and 28 were presented in Table 5. However, equation 28 had a low R^2 value showing a poor fitting while equation 27 was the best for fitting the Nusselt number for palm fruit mesocarp fibre.

Table 5: Constants in equation 27 and 28

Equation	Constants				
	a	b	c	d	R^2
27	1.24435	0.30106	0.66864	-	0.9998
28	0.95008	0.99738	-0.50597	1.00123	0.3772

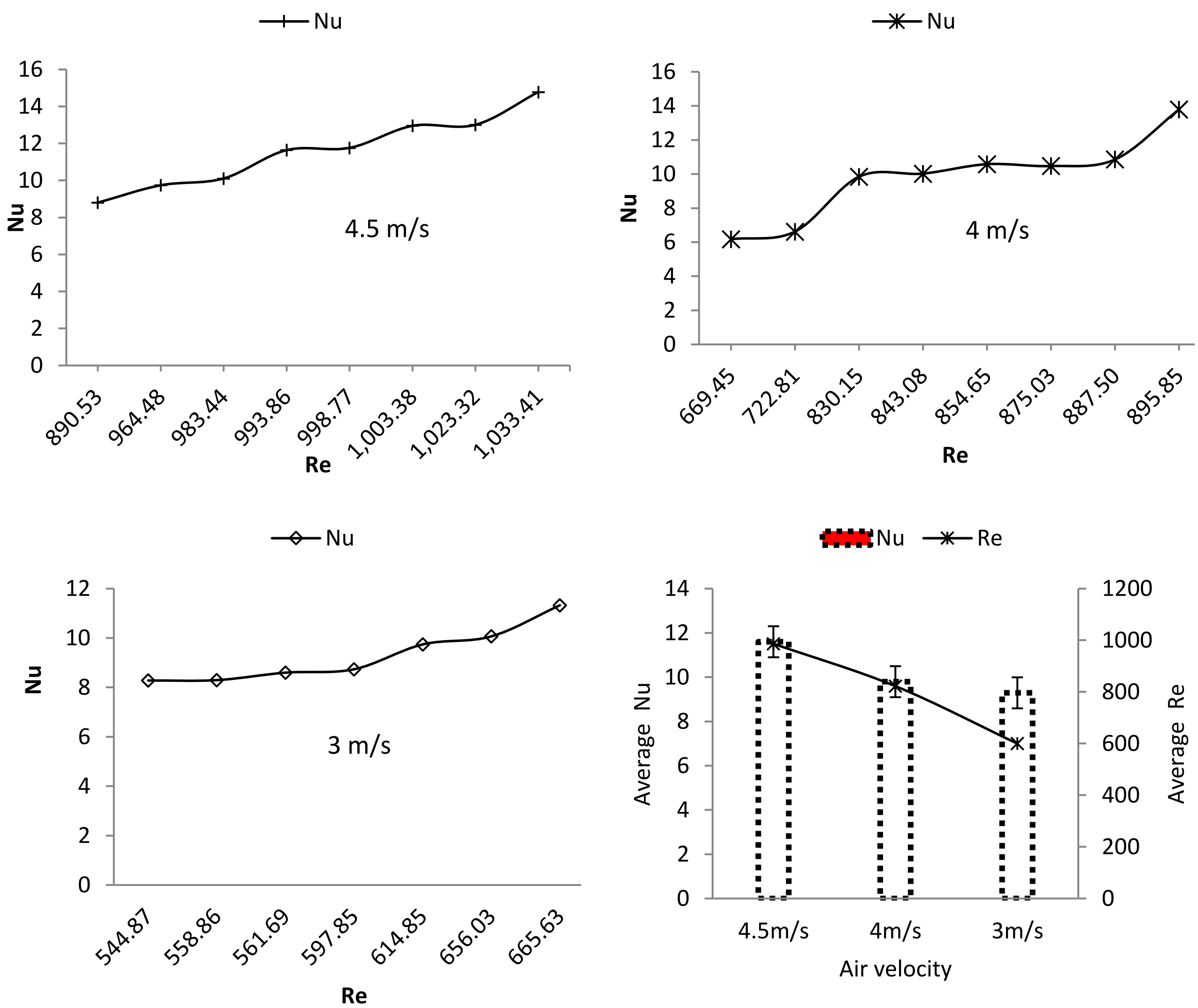

Figure 10: Non-dimensional heat transfer data correlations and their variations with air velocity

3.6 Respiratory heat dynamics of Amaranths

In storage agricultural products still respire due to senescence and generate heat according to equation 33 (Ndukwu, 2023)

$C_6H_{12}O_6 + 6O_2 \rightarrow +6CO_2 + 6H_2O$ + respiration heat 29

This heat generated is transferred to the surrounding air and can only be suppressed by low temperature and high humidity which partly depends on the type of wetting media performance. For the present experiment, the ambient temperature increased from morning time to noon period as shown in figure 5 before it decreased due to lower solar intensity. Thus cooler temperature was affected by this rise in temperature. Comparing Figures 11 and 5, you can see that a higher temperature drop was observed as the day goes by but it is not enough to lower the cooler temperature to suppress the respiratory heat. Therefore the respiratory heat load builds up and increases as shown in figure 11. For leafy vegetables like amaranths, the respiratory rate in storage is high. For all the air velocities the value ranged from 290.86 to 336.53 mg/kg.h. Although these values are high compared to unripe fruits but very low when compared to ripe Araze with a respiratory rate of 1283 mg/kg.h (USDA, 1986). However, the value obtained is within the range observed for vegetables like spinach, Asparagus and Broccoli storage at 15-20^{o}C (USDA,1986). Multi-regression correlations between the respiratory rate of amaranths and the cooler temperature were presented in equations 30-32 for 4.5, 4 and 3 m/s air velocity respectively

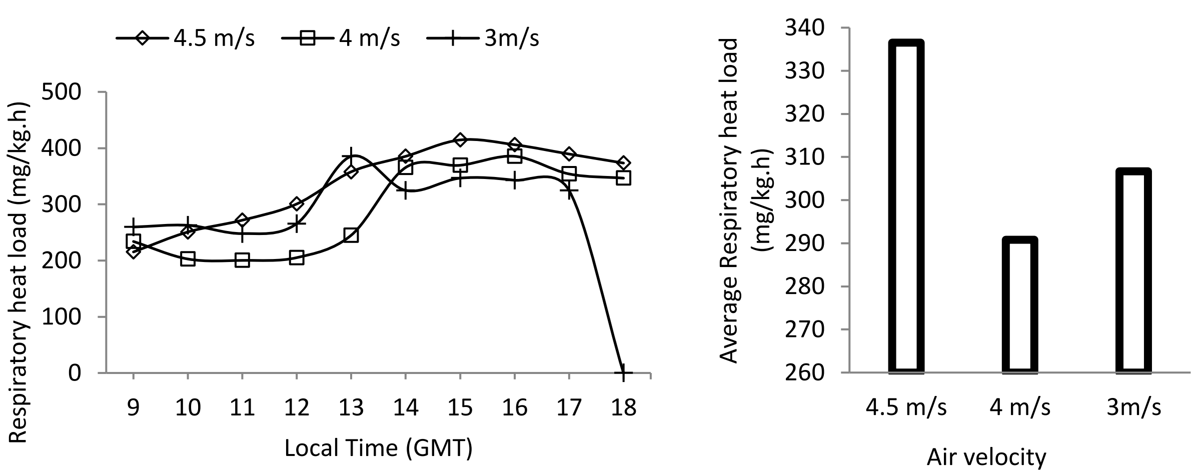

Figure 11: Variation in respiratory heat load of Amaranths at a different air velocity

$$q_{res} = 13.48\,T - 0.56T^2 + 0.03T^3 - 57.94 \qquad R^2=1.00 \qquad (30)$$

$$q_{res} = 12.48\,T - 0.51T^2 + 0.03T^3 - 50.52 \qquad R^2=1.00 \qquad (31)$$

$$q_{res} = 13.55\,T - 0.56T^2 + 0.03T^3 - 58.73 \qquad R^2=1.00 \qquad (32)$$

Conclusions

This paper investigates the forced convection heat transfer characteristics and resistance to airflow embodied in pressure drop for palm fruit mesocarp fibres used as wetting media in evaporative cooling storage of amaranths. The pressure drop and heat transfer data were evaluated parametrically from data generated in the field experiment at three air velocities using a standalone DEC. The palm fruit fibre offered very little resistance to airflow as the pressure drop per unit length was very low ranging from 5.29 to 7.62 Pa/m which presents it as a viable alternative in wetting media choices. The new constants developed for the correlations of heat transfer data and pressure drop fitted well with high R^2 values and can be used in the empirical prediction of the performance of the various parameters for palm fruit mesocarp fibres as wetting media in DEC systems. The Markel number and cooling efficiency showed inverse relationships as cooling time progressed. However, the average Merkel number varied between 0.16 to 0.19 while the average cooling efficiency varied between 56.43 to 65. 27 %. The Nusselt number values indicated a laminar flow for air passage through the media but the values increased with the Reynolds number. The obtained respiratory rate of amaranths in the cooler is higher compared to unripe fruits but it is within the range observed for vegetables like spinach, Asparagus and Broccoli storage at 15- 20ºC. Hence the respiration rate correlations developed with cooler temperatures can be used for other similar vegetables in DEC. For all the air velocities the value ranged from 290.86 to 336.53 mg/kg.h. Therefore, the DEC is suggested to be used as a pre-cooler for a very short period of storage of vegetables due to the high respiratory rate within the average cooler temperature for all airflow velocity.

References

1. Ndukwu, M.C, M. Simo-Tagne, E Inemesit, G. E. Akpan, M I Ibeh, D. O. Igbojionu, A. Tagne Tagne (2022a).The dynamics of respiratory heat load produced by orange using different biomass fibres as wetting materials in a direct evaporative cooling system. Biomass conversion and biorefinery. https://doi.org/10.1007/s13399-022-03694-5

2. Munoz, E.R., Duico, L.T., Martinez, S.M.S., Oliveria, I.K.A., Quiroz, N.A., Maria, D.J.R., (2017). Automated electronic evaporative cooler for fruits and vegetable preservation. Int. J. Eng. Sci. Res. Technol. 1–34.
3. Kasso, M., Bekele, A.,(2015). Post-harvest loss and quality deterioration of horticultural crops in Dire Dawa region, Ethiopia. J. Saudi Soc. Agric. Sci. 17.
4. Ndukwu M C, Manuwa S I. A techno-economic assessment for the viability of some waste as cooling pads in evaporative cooling system. Int J Agric & Biol Eng, 2015; 8(2): 151－158.
5. Ndukwu, M. C.; Manuwa, S. I.; Bennamoun, L.; Olukunle, O. J.; Abam, F. I. (2018). In-Situ Evolution of Heat and Mass Transfer Phenomena and Evaporative Water Losses of Three Agro-Waste Evaporative Cooling Pads: An Experimental and Modeling Study. Waste and Biomass Valorization, (), –. doi:10.1007/s12649-018-0315-9
6. Ndukwu M.C., M.I. Ibeh , E.C. Ugwu , D.O. Igbojionu , A.A. Ahiakwo, H. Wu (2022b). Evaluating coefficient of performance and rate of moisture loss of some biomass humidifiers materials with a developed simple direct stand-alone evaporative cooling system for farmers. Energy Nexus 8 (2022) 100146
7. Ndukwu M.C., M. I. Ibeh, G. E. Akpan, E. Ugwu, L. Akuwueke, L. Oriaku, Victor.E. Ihediwa, F.I. Abam, H.Wu, C.A. Kalu, A. E. Ben, J. Mbanasor (2023). Analysis of the influence of outdoor surface heat flux on the inlet water and the exhaust air temperature of the wetting pad of

a direct evaporative cooling system. Applied Thermal Engineering 226 (2023) 120292. https://doi.org/10.1016/j.applthermaleng.2023.120292

8. Lal Basediya A., D.V.K. Samuel, V. Beera, Evaporative cooling system for storage of fruits and vegetables - a review, J. Food Sci. Technol. 50 (3) (2011) 429–442, doi: 10.1007/s13197-011-0311-6
9. Ndukwu M.C, S.I. Manuwa, Review of research and application of evaporative cooling in the preservation of fresh agricultural produce, Int. J. Agric. Biol. Eng. 7 (5) (2014) 85–102 2014.
10. Liu Y, Y.G. Akhlaghi, X. Zhao, J. Li, Experimental and numerical investigation of a high-efficiency dew-point evaporative cooler, Energy Build. 197 (2019) 120130 2019.
11. Rao V.V, S.P. Datta, A feasibility assessment of single to multi/hybrid evaporative coolers for building air-conditioning across diverse climates in India, Appl. Therm. Eng. 168 (2020) 114813 2020 .
12. Ghani S, F. Bakochristou, E.M.A.A. ElBialy, S.M.A. Gamaledin, M.M. Rashwan, A. M. Abdelhalim, S.M. Ismail, Design challenges of agricultural greenhouses in hot and arid environments – a review, Eng. Agric. Environ. Food 12 (2019) 48–70, https://doi.org/10.1016/j.eaef.2018.09.004.
13. Nkolisa, N; Magwaza, Lembe S.; Workneh, Tilahun S.; Chimphango, Annie; Sithole, Nkanyiso J. (2019). Postharvest quality and bioactive properties of tomatoes (Solanum lycopersicum) stored in a low-cost and energy-free evaporative cooling system. Heliyon, 5(8), e02266–. doi:10.1016/j.heliyon.2019.e02266
14. Islam M.P., T. Morimoto, Evaluation of a new heat transfer and evaporative design for a zero energy storage structure, Sol. Energy 118 (2015) 469–484.
15. Ambuko J., F. Wanjiru, G.N. Chemining'wa, W.O. Owino, E. Mwachoni, Preservation of postharvest quality of leafy amaranth (*Amaranthus* spp.) vegetables using evaporative cooling, J. Food Qual. 2017 (2017) 1–7, doi: 10.1155/2017/ 5303156.
16. Dadhich S.M., H. Dadhich, R. Verma, Comparative study on storage of fruits and vegetables in evaporative cool chamber and ambient, Int. J. Food Eng. 4(2008), doi: 10.2202/1556-3758.1147'
17. Ndukwu M.C., Development of clay evaporative cooler for fruits and vegetable preservation, Agric. Eng. Int. CIGR J. 13 (1) (2011) 1–8.
18. He, S; Guan, Zhiqiang; Gurgenci, Hal; Hooman, Kamel; Lu, Yuanshen; M. Alkhedhair, Abdullah (2014). Experimental study of film media used for evaporative pre-cooling of air. Energy Conversion and Management, 87(), 874–884. doi:10.1016/j.enconman.2014.07.084
19. Yan, M; He, Suoying; Gao, Ming; Xu, Mengfei; Miao, Jiayu; Huang, Xiang; Hooman, Kamel (2020). Comparative study on the cooling performance of evaporative cooling systems using seawater and freshwater. International Journal of Refrigeration, (), S0140700720304072–. doi:10.1016/j.ijrefrig.2020.10.003
20. Dogramacı P.A., S. Riffat, G. Gan, D. Aydın, Experimental study of the potential of eucalyptus fibres for evaporative cooling, Renew. Energy 131 (2019) 250–260.
21. Aziz R.A., N.F. Zamrud, N. Rosli, Comparison of the cooling efficiency of cooling pad materials for an evaporative cooling system, J. Mod. Manuf. Syst. Technol. 01 (2018) 061–068.
22. Shekhar R., M.K. Chopra, R. Purohit, Design of a compact evaporative cooler to improve cooling efficiency and to evaluate the performance of different cooling pad materials, Int. J. Sci. Res. Dev. 4 (2016) 21–27.
23. Ndukwu M.C., Asoegwu S.N, 2010. Functional performance of a vertical-shaft centrifugal palm nut cracker.Res. Agr. Eng., *56*: 77–83.

24. Zhao Z, J. Gao, X. Zhu, Q. Qiu (2023). Experimental study of the corrugated structure of film packing on thermal and resistance characteristics of cross-flow cooling tower. International Communications in Heat and Mass Transfer 141 (2023) 106610
25. Yilmaz A (2010). Analytical calculation of wet cooling tower performance with large cooling ranges. J. of Thermal Science and Technology. 30, 2, 45-56, 2010
26. Milosavljevic, N., & Heikkilä, P. (2001). A comprehensive approach to cooling tower design. Applied Thermal Engineering, 21(9), 899–915. doi:10.1016/s1359-4311(00)00078-8
27. M. C. Ndukwu1 · S. I. Manuwa2 · L. Bennamoun3 · O. J. Olukunle2 · F. I. Abam. (2019). In-Situ Evolution of Heat and Mass Transfer Phenomena and Evaporative Water Losses of Three Agro-Waste Evaporative Cooling Pads: An Experimental and Modeling Study. Waste and Biomass Valorization 10:3185–3195. https://doi.org/10.1007/s12649-018-0315-9
28. Sohani, A., Zabihigivi, M., Moradi, M. H., Sayyaadi, H., & Hasani Balyani, H. (2017). A comprehensive performance investigation of cellulose evaporative cooling pad systems using predictive approaches. Applied Thermal Engineering, 110, 1589–1608. doi:10.1016/j.applthermaleng.2016.08.216
29. Engineering Toolbox.Moist Air - Density vs. Water Content and Temperature Density of the mix of dry air and water vapor - moist humid air. http/www.engineeringtoolbox.com/density-air-d_680.html, downloaded on 3/12/2023.
30. Ndukwu, M.C· M. Simo-Tagne · E. Inemesit, G E. Akpan, M. I. Ibeh, D. O. Igbojionu, A. Tagne Tagne (2023). The dynamics of respiratory heat load produced by orange using different biomass fibres as wetting materials in a direct evaporative cooling system. Biomass Conversion and Biorefinery.
https://doi.org/10.1007/s13399-022-03694-5
31. Becker, B.R.; Fricke, B.A. Simulation of Moisture Loss and Heat Loads in Refrigerated Storage of Fruits and Vegetables. New Dev. Refrig. Food Saf. Qual. 1996, 6, 210–221.
32. USDA. 1986. *The Commercial Storage of Fruits, Vegetables, and Florist and Nursery Stocks, Agricultural Handbook Number 66*, United States Department of Agriculture
33. Goshayshi H.R., J.F. Missenden, The investigation of cooling tower packing in various arrangements, Appl. Therm. Eng. 20 (2000) 69–80.
34. Malli A, Seyf HR, Layeghi M, Sharifian S, Behravesh H. Investigating the performance of cellulosic evaporative cooling pads. Energy Convers Manage 2011;52:2598–603.
35. Wang Y , X.Huang , J. Chu, M. Qu, T. Li, C. Dai (20222). Analysis of polishing waste ceramic foam packing in evaporative cooling. Applied Thermal Engineering 212 (2022) 118477
36. Franco A, Valera DL, Madueno A, Pena A. Influence of water and airflow on the performance of cellulose evaporative cooling pads used in Mediterranean greenhouse. Trans ASABE 2010;53:565–76.
37. Ma H, Y. Xie, Yu.Liu, Y. Liu, C. Hou, X. Luo, Q. Li (2022).The pressure drop characteristics of humid air outside staggered tube bundles in the evaporative cooling process. Nuclear Engineering and Design 395 (2022) 111855
38.